

Losing Weight: A KECK Spectroscopic Survey of the Massive Cluster of Galaxies RX J1347–1145¹

Judith G. Cohen² & Jean-Paul Kneib³

ABSTRACT

We present a sample of 47 spectroscopically confirmed members of RX J1347–1145, the most luminous X-ray cluster of galaxies discovered to date. With two exceptions, all the galaxies in this sample have red $B - R$ colors and red spectral indices, with spectra similar to old local ellipticals. Using all 47 cluster members, we derive a mean redshift of $\bar{z} = 0.4509 \pm 0.003$, and a velocity dispersion of $910 \pm 130 \text{ km s}^{-1}$, which corresponds to a virial mass of $4.4 \times 10^{14} h^{-1} M_{\odot}$ with an harmonic radius of $380 h^{-1} \text{ kpc}$. The derived total dynamical mass is marginally consistent with that deduced from the cluster's X-ray emission based on the analysis of ROSAT/ASCA images (Schindler *et al.* 1997), but not consistent with the more recent X-ray analyses of Allen (2000), Ettori, Allen & Fabian (2001) and Allen *et al.* (2002). Furthermore, the dynamical mass is significantly smaller than that derived from weak lensing (Fischer & Tyson 1997) and from strong lensing (Sahu *et al.* 1998). We propose that these various discrepant mass estimates may be understood if RX J1347–1145 is the product of two clusters caught in the act of merging in a direction perpendicular to the line of sight, although there is no evidence from the galaxy redshift distribution supporting this hypothesis. Finally, we report the serendipitous discovery of a lensed background galaxy at $z = 4.083$ which will put strong constraints on the lensing mass determination once its counter-image is securely identified.

Subject headings: galaxy: clusters: general — galaxy: clusters: individual (RX J1347–1145) — galaxies: fundamental parameters — intergalactic medium

¹Based in large part on observations obtained at the W.M. Keck Observatory, which is operated jointly by the California Institute of Technology, the University of California and NASA,

²Palomar Observatory, Mail Stop 105-24, California Institute of Technology, Pasadena, CA 91125

³Observatoire Midi-Pyrénées, 14 Av. E.Belin, 31400 Toulouse, France

1. Introduction

As the most massive gravitationally bound objects in the Universe, galaxy clusters are prime targets for studies of structure formation and evolution. In order to use these massive objects as cosmological tools, a good understanding of their mass distribution is required to relate the numerical simulation predictions to the observations. Because of their generic rarity, the most massive clusters constitute in principle the most sensitive cosmological probes, with the most distant ones providing the tightest constraints, specifically on the value of Ω_0 (e.g., Bahcall & Fan 1998; Ebeling et al. 2001). X-ray selection is currently the most favored technique for finding these massive systems in the Universe because of the very well defined selection criteria. However the most extreme clusters may also be the most unusual cases that may not be present in the current generation of numerical simulations of the Universe. Hence, precise understanding of the most massive clusters is very important in order to derive any useful cosmological constraint.

As an example, MS1054–0321, the highest redshift cluster in the EMSS, is a very massive cluster. Donahue *et al.* (1998) ascribed a virial mass of $7.4 \times 10^{14} h^{-1} M_\odot$ (for $\Omega_m = 1$) to MS1054–0321 based on both its X-ray temperature and a velocity dispersion from a sample of twelve spectroscopic members of $1360 \pm 450 \text{ km s}^{-1}$. However, even in this initial study of MS1054–0321, the presence of considerable substructure was noted. More recently, a careful weak lensing analysis using HST images by Hoeckstra, Franx & Kuijken (2000), a velocity dispersion analysis with a larger sample of spectroscopically confirmed cluster members (78 cluster members, giving $\sigma_v = 1150 \pm 97 \text{ km s}^{-1}$) by van Dokkum *et al.* (2000), and new *Chandra* observations (Jeltema *et al.* 2001) all seem to support a value for the virial mass of MS1054–0321 about a factor of two lower.

We focus in this paper on the cluster of galaxies RX J1347–1145 ($z=0.451$), discovered by ROSAT. This cluster is the most luminous X-ray cluster discovered to date (Schindler *et al.* 1995) with an intrinsic bolometric X-ray luminosity ⁴ of $L_{bol} = 50 \times 10^{44} h^{-2} \text{ ergs s}^{-1}$ and a gas temperature of $T_X = 9.3 \pm 1.0 \text{ keV}$ from ASCA observations (Schindler *et al.* 1997). The presumption that this is a high mass object is enhanced by the discovery of two reasonably bright long arcs with lengths of ~ 6 arcsec (see Sahu *et al.* 1998 for the lensing analysis) and by a clear detection of weak lensing (Fischer & Tyson 1997). More recently, Komatsu *et al.* (1999) and Pointecouteau *et al.* (2001) have respectively tried to estimate the cluster mass by the measure of the Sunyaev-Zeldovich (SZ) increment (resp. decrement) at submm (resp. mm) wavelengths.

⁴All published values have been adjusted to the common value of $H_0 = 100 \text{ km s}^{-1} \text{ Mpc}^{-1}$, and the explicit dependence on $h = H_0/100$ is given.

We present here Keck spectroscopy of galaxies in RX J1347–1145 which allow us to probe the dynamics of this massive cluster. Section 2 describes the observations and the spectral characteristics of the 47 cluster members. A detailed analysis of the spectra is carried out using spectroscopic indices in section 3. In section 4, we discuss the results in terms of the dynamical estimate of the mass of this cluster, and compare the derived mass to other mass estimates in section 5. Finally, in section 6, we discuss the discovery of a lensed galaxy at $z = 4.083$. Prospects for improving our understanding of the mass distribution of this cluster are discussed in the last section.

For consistency with earlier work, we adopt the cosmology $\Omega_m = 0.3$, $\Lambda = 0.0$ and $H_0 = 100h$ km/s/Mpc so that the angular scale at the distance of RX J1347–1145 is $3.67 h^{-1}$ kpc/arcsec. Were we to adopt a flat Universe with $\Lambda = 0.7$, the angular scale would increase by $\sim 10\%$ to 4.04 kpc/arcsec.

2. Keck Spectroscopy

Candidate member galaxies in the cluster RX J1347–1145 were first selected in 1998, as extended objects of appropriate brightness from a stacked R -band image (4×200 sec) taken with LRIS (Oke *et al.* 1995). Beginning in early 2000, we used a color image (made of a B and R -band image) to select candidates with suitably red $B - R$ color for spectroscopic observations. This significantly enhanced the efficiency of detecting cluster members rather than foreground or background galaxies. However, it has probably introduced a bias favoring the inclusion of elliptical galaxies in our sample. Three slitmasks were used with LRIS, one in 1998 ($t_{exp} = 2500$ s), one in 2000 ($t_{exp} = 2500$ s), and one in May 2001 ($t_{exp} = 2 \times 2500$ s). The 300 g/mm grating yielding a dispersion of 2.5Å/pixel with a 1.0 arcsec wide slit (projected width of 4.7 pixels) was used for all masks.

The spectra were reduced in a standard way using Figaro (Shortridge 1993) scripts.

Redshifts were determined by centroiding the CaII H and the K lines [JC], as well as using a cross correlation technique (*IRAF/RVSAO2.0* package) [JPK]. The results were indistinguishable within the errors. From this analysis, a sample of secure 46 members was isolated, with one additional probable cluster member (C47314_4511) whose spectrum was too noisy to yield an accurate redshift. However, the presence of a detectable 4000Å break strongly suggests that it belongs to the cluster. Five of the cluster galaxies have two independent spectra taken in different runs; these show no systematic redshift offsets.

The galaxy C47229_4519 has a spectrum very different from any other cluster member. It is, excluding the Western cD, the only cluster galaxy showing even weak [OII] 3727Å

emission, and its redshift ($z = 0.4392$) is slightly lower than all but one other cluster member. It is located in the outer part of RX J1347–1145 and has a blue $B - R$ color. We include it as a cluster member.

Altogether, the total number of spectroscopically confirmed galaxies in the close vicinity of RX J1347–1145 is 47. Figure 1 shows the velocity distribution centered on the cluster redshift. Note that there are no other galaxies in the spectroscopically observed sample with $0.41 < z < 0.52$.

Four galaxies (C47229_4519 included) are slightly offset in redshift compared to the main cluster redshift distribution. Perhaps they are either linked to the cluster infall region or are part of the large scale structure surrounding the cluster.

The two central cDs have approximately equal R -band luminosity, but display very different spectra. The Western cD galaxy, located at the X-ray peak, is an AGN and has been detected as a radio point source by the NVSS (Condon *et al.* 1998, Bauer *et al.* 2000). Its spectrum shows extremely strong [OII] 3727Å emission as well as emission at H β . Weaker emission at [OII] at 4959 and 5007Å as well as H γ and perhaps H δ is detected. These emission lines have been observed in the spectra of many giant elliptical galaxies sitting at the center of cooling flow clusters (*e.g.* Crawford *et al.* 1995).

Absolute astrometric calibration of the field was carried out using the USNO-A V2.0 (Monet *et al.* 1998). Table 1 gives the location and redshifts for the cluster members, with total R magnitudes from the best fit large aperture results from the FOCAS package described in Valdes (1989). Table 2 lists the non-members observed, consisting of 22 field galaxies and their galaxy spectral classification according to the system of Cohen *et al.* (1999), as well as stars, some of which were used to align the slitmasks. Figure 2 shows the R -band image of the central part of RX J1347–1145, where we have indicated the galaxies in our sample with their redshifts.

3. Spectral Indices

To illustrate that the members of the cluster of galaxies RX J1347–1145 are typical early type galaxies, we have measured the strengths of various spectral features, the strength of emission in the 3727Å line of [OII], and the absorption in the 3968Å line of CaII as well as an index for the strength of the 4000Å break. Table 3 lists the specific bandpasses used to define each of these indices. The results as a function of total R mag are shown in Figures 3, 4 and 5. The possible non-member galaxy C47229_4519 is included in each of these figures.

Aside from the AGN and the possible non-member galaxy, the remaining 45 members of RX J1347–1145 show no evidence for emission in the 3727Å line of [OII] (see Figure 3). Repeat measurements suggest an accuracy of $\pm 3\text{\AA}$ for the fainter galaxies in our sample. The same two galaxies stand out from the rest of the sample in Figure 4, where they display Balmer jumps considerably smaller than the majority of the cluster galaxies, and in Figure 5, where they have less absorption in the 3933Å line of Ca II. All of this is to be expected given that one of these galaxies is an AGN and the second appears to be very blue, presumably from ongoing star formation.

4. Velocity Dispersion and Virial Mass

The velocity dispersion was computed using the bi-weight algorithm of Beers, Flynn & Gebhardt (1990), as it is very robust to the presence of outliers. An instrumental uncertainty of $\pm 100 \text{ km s}^{-1}$ in the rest frame is assumed for all measurements. The bi-weight estimator gives $\sigma_v = 910 \pm 130 \text{ km s}^{-1}$ using the 47 known members of the cluster RX J1347–1145. A slightly smaller value ($\sigma_v = 820 \pm 110 \text{ km s}^{-1}$) is obtained using a classical 3-sigma clipping algorithm (which has the effect of removing the four galaxies discussed in section 2, which are slightly offset from the main distribution). Hereafter, we adopt a velocity dispersion of 910 km s^{-1} for this cluster. Assuming that the cluster follows the $\sigma-T_X$ relation (*e.g.* Girardi *et al.* 1996), we derive an X-ray temperature of $T_X = 5.1 \pm 1.2 \text{ keV}$.

The central redshift for the velocity distribution is $z = 0.45095$. The redshift of the Eastern and Western cDs are respectively $z = 0.4506$ and $z = 0.4515$, both of which correspond to rest frame radial velocities that are within 100 km s^{-1} of the central value. Therefore, taking into account the measured uncertainties, they are both consistent with being at rest at the dynamical center (in the line of sight direction); however we can not speculate on any transverse velocities.

The centroid of the galaxy distribution appears to be closer to the Western cD, rather than to the point half way between the two cDs, which are 18 sec apart. Thus, we adopt the position of the AGN as the dynamical center of the cluster, as it is also corresponds to the X-ray peak.

As Figure 1 shows, the velocity distribution appears to be that of a Gaussian. A K-S test shows that the probability that the observed velocity distribution for the members of the cluster RX J1347–1145 and the fit Gaussian are the same exceeds 98%. There is no evidence in our sample of any deviation of the distribution of the radial velocities from a single Gaussian.

We computed the harmonic radius R_h (e.g., Saslow 1985, Nolthenius & White 1987) from our spectroscopic cluster members as

$$R_h = D_A(\bar{z}) \frac{\pi}{2} \frac{N_m(N_m - 1)}{2} \left(\sum_i \sum_{j > i} \theta_{ij}^{-1} \right)^{-1}, \quad (1)$$

where θ_{ij} is the angular distance between galaxies i and j , N_m is the number of cluster members, and $D_A(\bar{z})$ is the angular diameter distance at the mean cluster redshift \bar{z} . The cluster virial mass can then be estimated as

$$M_V = \frac{6\sigma^2 R_h}{G}. \quad (2)$$

We found an harmonic radius of $R_h = 380h^{-1}$ kpc and a mass $M_V = 4.4_{-1.2}^{+1.4} 10^{14}h^{-1} M_\odot$. This value is somewhat larger than that derived from the measured $\sigma(v)$ alone using the fits of Arnaud & Evrard (1999) to the simulations of Evrard *et al.* (1996) for the mass within a region whose density is 200 times the critical density, $M = 2.9 \times 10^{14}h^{-1} M_\odot$.

5. Comparison of the Virial Mass With Other Mass Estimators

Measurements of cluster masses deduced from X-ray emission are based on the assumption that the X-ray emitting gas is in hydrostatic equilibrium with the gravitational potential of the cluster. With a constant $T_X = 9.3 \pm 1.$ keV temperature measured from ASCA data, Schindler *et al.* (1997) deduced from the ROSAT images of RX J1347–1145 a gas mass of $1.0 \times 10^{14} h^{-1} M_\odot$ and a total binding mass of $2.9 \times 10^{14} h^{-1} M_\odot$ within a radius of $500 h^{-1}$ kpc.

X-ray mass determinations are usually given as a mass enclosed within a specified radius. We adopt a power law $\rho(r) \propto r^{-x}$ for the spatial distribution of galaxies within a cluster to determine the conversion between the harmonic radius and the outer radius, r_{max} . Kent & Gunn (1982) found $x \sim 3$ is the appropriate power law to characterize the distribution of galaxies in the Coma Cluster, and we adopt that value. Ignoring a central core extending to $r = 0.05r_{max}$, the harmonic radius is then $0.49r_{max}$, and this fraction decreases for an even steeper density drop-off or as more of the core is included. Thus the area surveyed by our optical sample, with $R_h = 380h^{-1}$ kpc, is roughly comparable to an X-ray mass specified within $1h^{-1}$ Mpc.

RX J1347–1145 has a large cooling flow ($\gtrsim 1000 M_\odot/\text{year}$). Its high luminosity and mass are confirmed by the recent analysis of BeppoSAX observations of this cluster by Ettori *et al.* (2001), who focus on the cluster gas temperature and the impact of the large cooling flow in its central region. They find, confirming Allen (2000), a gas temperature of ~ 14

keV, but not as large as the very high value of $26.4^{+7.8}_{-12.3}$ keV of Allen (1998), who points out the importance of proper treatment of the cooling flow to the value of the mass near the center of the cluster. Furthermore Molendi & Pizzolato (2001) present XMM observations which do not find evidence for multi-phase gas in several nearer clusters of galaxies with strong cooling flows.

The cooling flow, the possible presence of substructure, the residual heating effects from possible previous mergers, may all be playing a role here. Sarazin (2001) reviews the theory of cluster mergers, while Ritchie & Thomas (2001) demonstrate through hydrodynamic simulations that the X-ray luminosity and/or temperature may be strongly enhanced in merging clusters. Schuecker *et al.* (2001) find that $\sim 50\%$ of a sample of the nearest clusters of galaxies show evidence for substructure, presumably arising from recent mergers, based on their ROSAT images.

The recent *Chandra*/ACIS RX J1347–1145 image (a 20 ksec exposure extracted from the *Chandra* archive) shows an extended source whose center coincides with the AGN (the Western of the two central cDs) to within 0.8 arcsec (the relative astrometry was checked using a single faint X-ray point source at $\alpha=13h47m36.98s$ $\delta = -11d44m09.0s$ (J2000) that was identified with a faint field galaxy). Taking into account all the astrometric uncertainties, the Western cD and the X-ray peak are consistent with both being at exactly the same position. The contribution of the AGN itself to the total X-ray flux is likely to be small. A more detailed analysis of these data by Allen *et al.* (2002) leads again to a very high X-ray temperature, $T_X = 12.7 \pm 1$ keV. The emission (shown as an overlay in Figure 2) is to first order circularly symmetric with a probable extension to the SE and extends to a radius $\lesssim 240$ arcsec, a region comparable in size to that of the optical spectroscopic sample presented here. A similar SE extension is seen in the SZ decrement map of Pointecouteau *et al.* (2001); it is in fact the most prominent peak of the SZ map, arguing for a very high temperature for this clump as well as in the map of Komatsu *et al.* (2001). The SZ results of Pointecouteau *et al.* (2001) leads to projected gas mass of $1.9 \pm 0.1 \times 10^{13} h^{-5/2} M_\odot$ within an angular radius of 74 arcsec (272 h^{-1} kpc) assuming a spherical distribution for the gas. This value is in reasonable agreement with the X-ray determination for the gas mass in this cluster.

The virial mass of RX J1347–1145 can be compared to the mass derived from weak lensing of Fischer & Tyson (1997) of $1.1 \pm 0.3 \times 10^{15} h^{-1} M_\odot$ within the same $1 h^{-1}$ Mpc radius for this cluster. Assuming an isotropic velocity distribution, the weak lensing results translate into a predicted velocity dispersion of 1500 ± 160 km s $^{-1}$ (Fischer & Tyson 1997). However, the seeing for the images of this cluster from the CTIO 4-m telescope with the prime focus CCD camera analyzed by Fischer & Tyson was 1.2 arcsec, and the seeing was spatially

variable across the field. There was noticeable PSF anisotropy due to several known technical problems which have since been resolved; see Fischer & Tyson for a detailed description of these issues and their attempt to overcome elliptical PSFs with sophisticated software. It is therefore not too surprising given all these problems that their attempt may have resulted in an overestimation of the mass.

The strong lensing analysis for one of the central arcs by Sahu *et al.* (1998) also suggests a very high mass. They derive the projected mass within the radius of the arcs, 38 arcsec (140 h^{-1} kpc), and obtain $3.4 \times 10^{14} h^{-1} M_{\odot}$, which corresponds to roughly $\sigma = 1300 \text{ km s}^{-1}$ for a singular isothermal sphere. Note, however, that this mass estimate assumes that the $z = 0.81$ arc seen in RX J1347–1145 is located at the Einstein radius, which may be an incorrect assumption as no multiple images were identified in this analysis. Thus the derived strong lensing mass estimate should be considered as an upper limit.

Table 4 summarizes the current discrepant situation, in terms of the velocity dispersion, X-ray temperature or total projected mass within some specified radius. The various measurements have been converted assuming the $T_X - \sigma$ relation of Girardi *et al.* (1996); the values so derived are given in brackets in columns 3 and 4 of this table.

6. Probable Detection of a Lensed Object at $z = 4.083$

During the spectroscopic survey to locate members of the cluster of galaxies RX J1347–1145, we serendipitously found an object (O47332_4511) with a strong emission line at 6177Å and essentially no continuum blue-ward of this line. Identifying the line with Lyman- α and the lack of blue continuum as the Lyman limit gives a redshift of $z = 4.083$ (Figure 6), and the equivalent width of Lyman- α is $\sim 45 \text{ \AA}$. This object, with $R = 23.7$ (although the very strong emission falls within the R bandpass, it should not contribute to the R -band flux by more than 10%) is 38 arcsec East of the Western cD. Its image is a point source on the STIS image (Figure 6).

With the aid of simple lensing mass models (following the precepts of Kneib *et al.* 1996), we have identified two faint objects with the appropriate morphology that might be counterparts of this $z = 4.083$ object: O47283_4517 and O47300_4517 (objects A and B respectively, marked in Fig. 2). These models assume that the $z = 4.083$ object is multiply imaged by the cluster, but this need to be confirmed in the future; at present we lack the necessary color and spectroscopic information for objects A and B. If we accept either of these two objects marked in Figure 2 as a possible counter-image of the $z = 4.083$ object, a strong lensing analysis suggests a much smaller total projected mass within a 38 arcsec (140

h^{-1} kpc) radius centered on the Western cD compared to the previous lensing analysis. We find a mass of $1.4 \times 10^{14} M_{\odot}$ for O47300_4517 (which would correspond to $\sigma \sim 850 \text{ km s}^{-1}$ for a singular isothermal sphere) and $1.9 \times 10^{14} M_{\odot}$ for O47283_4517 ($\sigma \sim 1000 \text{ km s}^{-1}$ for a similar model). Both mass models are made of two massive cluster scale components centered respectively on each of the two central cDs. The latter case (object A) is more likely to be correct, as in the former, the observed flux ratio between the two images is different than the one predicted by the lens model. Both of these mass estimates are much smaller than the previous weak or strong lensing estimates and both are consistent with our dynamical estimate.

7. Discussion

Based on 47 spectroscopically confirmed cluster members, we have determined the virial mass of RX J1347–1145, the most luminous X-ray cluster known. This mass estimates is much lower than the most recent X-ray, SZ and lensing mass estimates. Note that the case of RX J1347–1145 is not unique and that a number of massive clusters are poorly understood. All methods of determining the mass of a cluster of galaxies suffer some bias, which if understood should allow us to understand cluster physics. We suggest that the extremely high X-ray luminosity of this cluster does not denote an extremely high mass, but rather that we may be witnessing an unusual merger of two clusters.

How accurate is our dynamical mass estimates? The lack of velocity structure in the velocity histogram seems to argue that there is no sub-structure in the line of sight direction. Moreover, the fact that most member are red ellipticals argues that the dynamical estimate is a secure estimate of the projected mass. However, the much higher mass inferred from recent X-ray and SZ analyses as well as the complex structure reported in their maps may most easily be understood if the cluster is currently suffering a major merger in the plane of the sky (hence barely affecting the dynamical mass estimate). The probability that such a collision might occur is proportional to the solid angle subtended by a collision “primarily in the plane of the sky”, which, for relative velocity vectors $\pm 30^\circ$ from the plane of the sky, is 50%.

Such a merger occurring primarily in the plane of the sky could explain the origin of the various discrepant temperature measurements for this cluster. For multiple merging clumps along a line of sight, the weak lensing signal adds linearly. Hence, irrespective of whether RX J1347–1145 is in the process of a merger, the weak lensing mass estimate should yield the correct total mass for the cluster. The dynamical mass estimate, however, will be biased toward the mass of the larger clump, at least until the merger is complete and the galaxy

orbits have virialized to the new total cluster mass. Given the substantial uncertainties on the weak lensing mass measurement of Fischer & Tyson (1997), it is just possible to reconcile the values given in Table 4 for the dynamical and weak lensing mass if the masses of the two hypothetical clumps (M_1 and M_2 , with $M_2 \leq M_1$) are comparable, with $0.7 < M_2/M_1 \leq 1$.

Turning to the X-ray measurements, the observed values of T_X are very high compared to our dynamical galaxy velocity dispersion. It is likely that the X-ray emitting gas virializes more rapidly in the course of a merger than do the galaxies, and hence might reflect the new total mass of the cluster before the galaxy velocity dispersion would do so. To reproduce the observations with a merger hypothesis, we require equal mass clumps⁵, a merger primarily in the plane of the sky, and also a time chosen so that the X-ray gas has virialized to the new cluster total mass but the galaxies have not. Even with this somewhat contrived scenario, it is still not possible to reconcile our dynamical mass with the recent X-ray analyses unless the uncertainties in the various measurements of T_X have been underestimated. Substantial non-thermal X-ray emission, presumably from shocks associated with the hypothesized merger, is still required to explain the X-ray observations of RX J1347–1145.

This merger assumption, although attractive, needs to be confirmed. As indicated above, in our present sample of 47 spectroscopically confirmed cluster members, there is no evidence for a merger. A detailed 3D analysis, such as that of Czoske *et al.* (2001) for the Cl0024+1654 cluster, would require a sample of ~ 200 spectroscopic members of the cluster. If deep HST/ACS data are obtained, we will also be able verify candidate counter-images and to model accurately the lensing distortion and multiple images to provide additional constraints on the mass distribution within RX J1347–1145.

Large scale programs to search for distant clusters of galaxies are underway using both X-ray and optical techniques to find distant clusters. We need to understand how to measure the mass of clusters accurately before the comparison of cluster samples at low and high redshift can be used to constrain cosmology with any degree of precision. The massive, X-ray luminous cluster RX J1347–1145 is a perfect case to try to understand what has gone wrong and how to make it right.

The entire Keck/LRIS user community owes a huge debt to Jerry Nelson, Gerry Smith, Bev Oke, and many other people who have worked to make the Keck Telescope and LRIS a reality. We are grateful to the W. M. Keck Foundation for the vision to fund the construction of the W. M. Keck Observatory. The authors wish to extend special thanks to those of

⁵We assume that the probability of a merger involving three or more equal mass clumps is so low that we can ignore such events.

Hawaiian ancestry on whose sacred mountain we are privileged to be guests. Without their generous hospitality, none of the observations presented herein would have been possible. The archival STIS data was retrieved from the STScI archive and was taken with the NASA/ESA Hubble Space Telescope, which is operated by STScI for the Association of Universities for Research in Astronomy, Inc., under NASA contract NAS5-26555. We are grateful to Oliver Czoske, Phil Fisher and Piet van Dokkum for useful discussions and suggestions. JPK thanks the CNRS for support.

REFERENCES

Allen, S. W., 1998, MNRAS, 296, 392

Allen, S. W., 2000, MNRAS, 315, 269

Allen, S.W., Schmidt, R.W., Fabian, A.C. & Ettori, S., 2002, Contribution to Moriond Meeting

Arnaud, M. & Evrard, G., 1999, MNRAS, 305, 631

Bahcall, N. A. & Fan, X. H., 1998, ApJ, 504, 1

Bauer, F.E., Condon, J.J., Thuan, T.X. & Broderick, J.J., 2000, ApJS, 129, 547

Beers, T. C., Flynt, K. & Gebhardt, K., 1990, AJ, 100, 32

Cohen, J. G., Hogg, D. W., Pahre, M. A., Blandford, R., Shopbell, P. L. & Richberg, K., 1999, ApJS, 120, 171

Crawford, C. S., Edge, A. C., Fabian, A. C., Allen, S. W., Bohringer, H., Ebeling, H., McMahon, R. G., & Voges, W. 1995, MNRAS, 274, 75

Condon, J.J., Cotton, W.D., Greisen, E.W., Yin, Q.F., Perley, R.A., Taylor, G.B. & Broderick, J.J., 1998, AJ, 115, 1693

Czoske, O., Moore, B., Kneib, J. P., Soucail, G., 2000, A&A, submitted, (astro-ph/0111118)

Donahue, M., Voit, G.M., Gioia, I., Luppino, G., Hughes, J.P. & Stocke, J.T., 1998, ApJ, 502, 550

Ebeling, H., Edge, A.C. & Henry, J.P., 2001, ApJ, 553, 668

Ettori, S., Allen, S.W. & Fabian, A.C., 2001, MNRAS, 322, 187

Evrard, G., Metzler, C.A. & Navarro, J.F., 1996, ApJ, 469, 494

Fischer, P. & Tyson, J.A., 1997, AJ, 114, 14

Girardi, M., Fadda, D., Giuricin, G., Mardirossian, F. & Mezzetti, M., 1996, ApJ, 457, 61

Hoekstra, H., Franx, M. & Kuijken, K., 2000, ApJ, 532, 88

Irwin, J. A. & Bregman, J. N., 2000, ApJ, 538, 543

Jeltema, T.E., Canizares, C.R., Bautz, M.W., Malm, M.R., Donahue, M. & Garmire, G.P., 2001, ApJ (in press) (Astro-ph/0107314)

Kent, S. M. & Gunn, J. E., 1982, AJ, 87, 945

Kneib, J. P., Ellis, E. S., Smail, I., Couch, W. J. & Sharples, R. M., 1996, ApJ, 471, 643

Komatsu, E. *et al.*, 1999, ApJ, 516, L1

Komatsu, E. *et al.*, 2001, PASJ, 53, 57

Markevitch, M., 1997, ApJ, 483, L17

Molendi, S. & Pizzolato, F., 2001, ApJ (in press) (Astro-ph/0106552)

Monet, D.G. *et al.*, 1998, USNO CD-ROM

Nolthenius, R. & White, S.D.M., 1987, MNRAS, 235, 505

Oke, J. B., Cohen, J. G., Carr, M., Cromer, J., Dingizian, A., Harris, F. H., Labrecque, S., Lucinio, R., Schaal, W., Epps, H., & Miller, J. 1995, PASP, 107, 307

Pointecouteau, E., Giard, M., Benoi, A., Desert, F.X., Bernard, J.P., Coron, N. & Lamarre, J.M., 2001, ApJ, 552, 42

Ritchie, B.W. & Thomas, P.A., 2001, MNRAS, in press (Astro-ph/0107374)

Sahu, K. *et al.*, 1998, ApJ, 492, L125

Sarazin, C.L., 2001, to appear in *Merging Processes in Clusters of Galaxies*, ed. L.Feretti, I.M.Gioia & G.Giovannini, (Dordrecht: Kluwer)

Saslow, W.C., 1985, *Gravitational Physics of Stellar and Galactic Systems*, Cambridge University Press

Schuecker, P., Böhringer, H., Reiprich, T.H. & Feretti, L., 2001, A&A (in press) (Astro-ph/0109030)

Schindler, S., Guzzo, L., Ebeling, H., Böhringer, H., Chincarini, G., Collins, C.A., DeGrandi, S., Neumann, D.M., Briel, U.G., Shaver, P. & Vettolani, P., 1995, A&A, 299, L9

Schindler, S., Hattori, M., Neumann, D.M. & Böhringer, H., 1997, A&A, 317, 646

Shortridge, K., 1993, *The Figaro 2.4 Manual*

Valdes, F., 1989, in *First ESO/ST-EF Data Analysis Workshop*, ed. P.J.Grosbol, F.Murtagh & R.W. Warmels

van Dokkum, P.G., Franx, M., Fabricant, D., Illingworth, G.D. & Kelson, D.D., 2000, ApJ, 541, 95

Table 1. Properties of Members of RX J1347–1145

Galaxy ID ^a	<i>z</i>	<i>R</i> (Mag)	Galaxy ID ^a	<i>z</i>	<i>R</i> (Mag)
C47223_4714	0.4494	21.98	C47230_4432	0.4575	21.82
C47236_4646	0.4560	21.34	C7238_4437	0.4503	22.16
C47243_4419	0.4410	22.16	C47251_4429	0.4532	21.61
C47251_4556	0.4460	21.32	C47254_4530	0.4490	21.29
C47261_4521	0.4502	21.25	C47265_4528	0.4604	21.10
C47268_4342	0.4480	21.82	C47269_4424	0.4457 ^b	21.34
C47272_4543	0.4545	20.28	C47274_4556	0.4575	21.08
C47278_4553	0.4465	20.31	C47280_4551	0.4485	20.68
C47280_4454	0.4556 ^b	21.18	C47290_4600	0.4534	20.90
C47296_4450	0.4369 ^b	21.32	C47299_4456	0.4488	21.63
C47300_4519	0.4662	21.42	C47306_4509 ^c	0.4515	18.52
C47307_4319	0.4526	21.26	C47308_4526	0.4483	22.11
C47314_4511	... ^e	21.64	C47315_4510	0.4488	21.86
C47318_4511 ^d	0.4506	18.57	C47319_4507	0.4466	20.74
C47319_4616	0.4533	22.01	C47321_4352	0.4510	20.80
C47322_4518	0.4465	21.33	C47323_4709	0.4550	21.53
C47324_4350	0.4646	20.30	C47324_4504	0.4450	20.77
C47327_4513	0.4518 ^b	22.01	C47328_4614	0.4460	21.00
C47341_4452	0.4470 ^b	22.08	C47348_4501	0.4499	20.97
C47357_4502	0.4474	21.48	C47369_4434	0.4481	21.12
C47375_4447	0.4512	21.33	C47382_4444	0.4495	19.72
C47384_4435	0.4523	21.41	C47395_4428	0.4579	21.84
C47400_4533	0.4443	22.08	C47408_4523	0.4528	21.87
C47417_4449	0.4557	20.02	C47232_4518 ^f	0.4392	21.81

^aGalaxy names are based on their coordinates, Cxxyyy_wwzz has the position 13 xx yy.y –11 ww zz, epoch J2000.

^bThere are two independent spectra for this galaxy.

^cThis is the Western of the two central cDs.

^dThis is the Eastern of the two central cDs.

^eGalaxy on extreme edge of slit. Spectrum shows this is a cluster member, but redshift not sufficiently accurate to use for vel. dispersion.

^fProbable member.

Table 2. Redshift for Non-Members In This Field

Galaxy ID ^a	<i>R</i>	<i>z</i>	Spec. Type ^b	Galaxy ID ^e	<i>R</i>	<i>z</i>	Spec. Type ^b
	(Mag)				(Mag)		
O47234_4513	20.10	0.253	\mathcal{E}, \mathcal{I}	O47240_4633	20.99	0.614	\mathcal{E}, \mathcal{I}
O47244_4604	> 23	0.607	\mathcal{E}	O47259_4441	20.38	0.695	\mathcal{I}
O47265_4528	20.92	0.299	\mathcal{A}	O47274_4351	20.88	star	\mathcal{M}
O47276_4555	21.34	0.101	\mathcal{E}	O47291_4329	21.49	star	\mathcal{M}
O47296_4426	21.28	star	\mathcal{M}	O47314_4551	20.53	0.384	\mathcal{A}
O47326_4602	20.90	star	\mathcal{M}^c	O47332_4511	23.7	4.083	\mathcal{E}
O47332_4540	21.52	0.606	\mathcal{I}	O47335_4623	20.68	star	\mathcal{S}
O47335_4713	21.30	star	\mathcal{M}	O47339_4451	23.24	0.906	\mathcal{E}
O47346_4533	21.78	0.315	\mathcal{A}	O47346_4643	21.52	star	\mathcal{S}
O47354_4645	22.11	0.399	\mathcal{E}, \mathcal{I}	O47376_4706	23.03	0.400	\mathcal{E}
O47380_4821	22.05	0.721	\mathcal{E}	O47390_4552	21.42	0.183	\mathcal{E}, \mathcal{I}
O47390_4603	21.42	0.578	\mathcal{A}	O47393_4351	21.25	0.348	\mathcal{E}, \mathcal{I}
O47410_4253	20.87	0.348	\mathcal{A}	O47411_4340	19.70	0.348	\mathcal{A}
O47419_4449	21.12	0.539	\mathcal{E}, \mathcal{I}	O47455_4853	22.18	0.543	\mathcal{E}, \mathcal{I}
O47480_4514	21.55	0.361	\mathcal{E}, \mathcal{I}				

^aObject names are based on their coordinates, Cxxyyy-wwzz has the position 13 xx yy.y –11 ww zz, epoch J2000.

^bThe system of galaxy spectral types used is described in Cohen *et al.* (1999).

^cThis object has the spectrum of a M subdwarf.

Table 3. Wavelengths for the Line Indices

Feature Name	Feature (Å)	Blue Continuum (Å)	Red Continuum (Å)
3727Å [OII] Emission	3712 – 3742	0.5(3713 – 3741)	0.5(3742 – 3801)
3933Å Ca II Absorption	3918 – 3948	0.4(3500 – 3670)	0.6(4030 – 4090)
D4000 (Break) ^a	...	3850 – 3950	4000 – 4100

^aThis index is the ratio of the average flux in the shorter wavelength bandpass to that in the longer.

Table 4. Mass Indicators For the Cluster of Galaxies RX J1347–1145

Reference	Method	σ (km s $^{-1}$)	T_X (keV)	Mass (10 14 M $_{\odot}$)	Radius (h $^{-1}$ kpc)
X-ray					
Schindler <i>et al.</i> (1997)	(ROSAT/ASCA)	[1320±100]	9.3±1.0	2.9 / 8.5	500 / 1500
Allen (1998)	(ROSAT/ASCA)	[2500 $^{+420}_{-800}$]	26.4 $^{+7.8}_{-12.3}$	36 $^{+11}_{-17}$	1000
Allen (2000)	(ROSAT/ASCA)	1850 $^{+270}_{-500}$	10.4 – 26.4	...	880
Ettori <i>et al.</i> (2001)	(BeppoSax)	[1635 – 2250]	13.2 – 22.3	...	1300 ^a
Allen <i>et al.</i> (2002)	(Chandra)	[1595±75]	12.7±1.0	...	1000
Lensing					
Fischer & Tyson (1997)	weak lensing	1500±220	[11.5±2.8]	11±3	1000
Sahu <i>et al.</i> (1998)	strong lensing	1300	[9.1]	3.4	140
This Paper	strong lensing	850 / 1000	[4.5 / 5.9]	1.4 / 1.9	140
Galaxy $\sigma(v)$					
This Paper	galaxy $\sigma(v)$	910±130	[5.1±1.2]	4.4 $^{+1.4}_{-1.2}$	$R_h = 380$

^aThis is the radius of the aperture used, but the instrumental PSF is very broad.

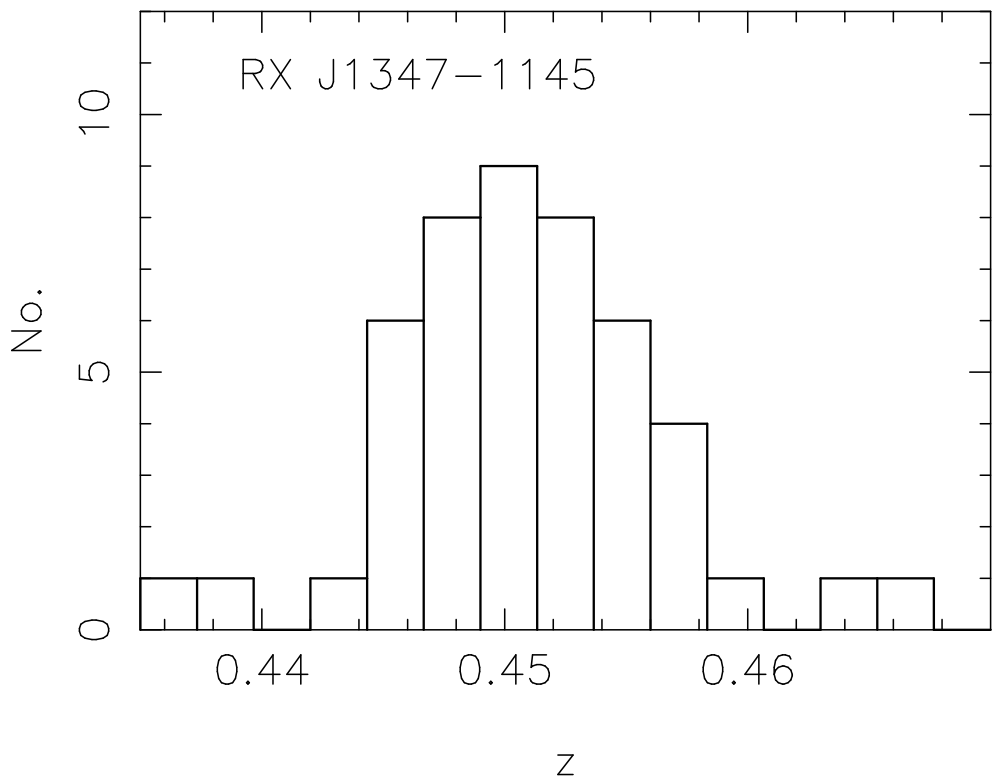


Fig. 1.— The histogram of velocities for 47 spectroscopically confirmed members of the massive cluster of galaxies RX J1347–1145 is shown. There are no other galaxies in the sample with $0.41 < z < 0.52$.

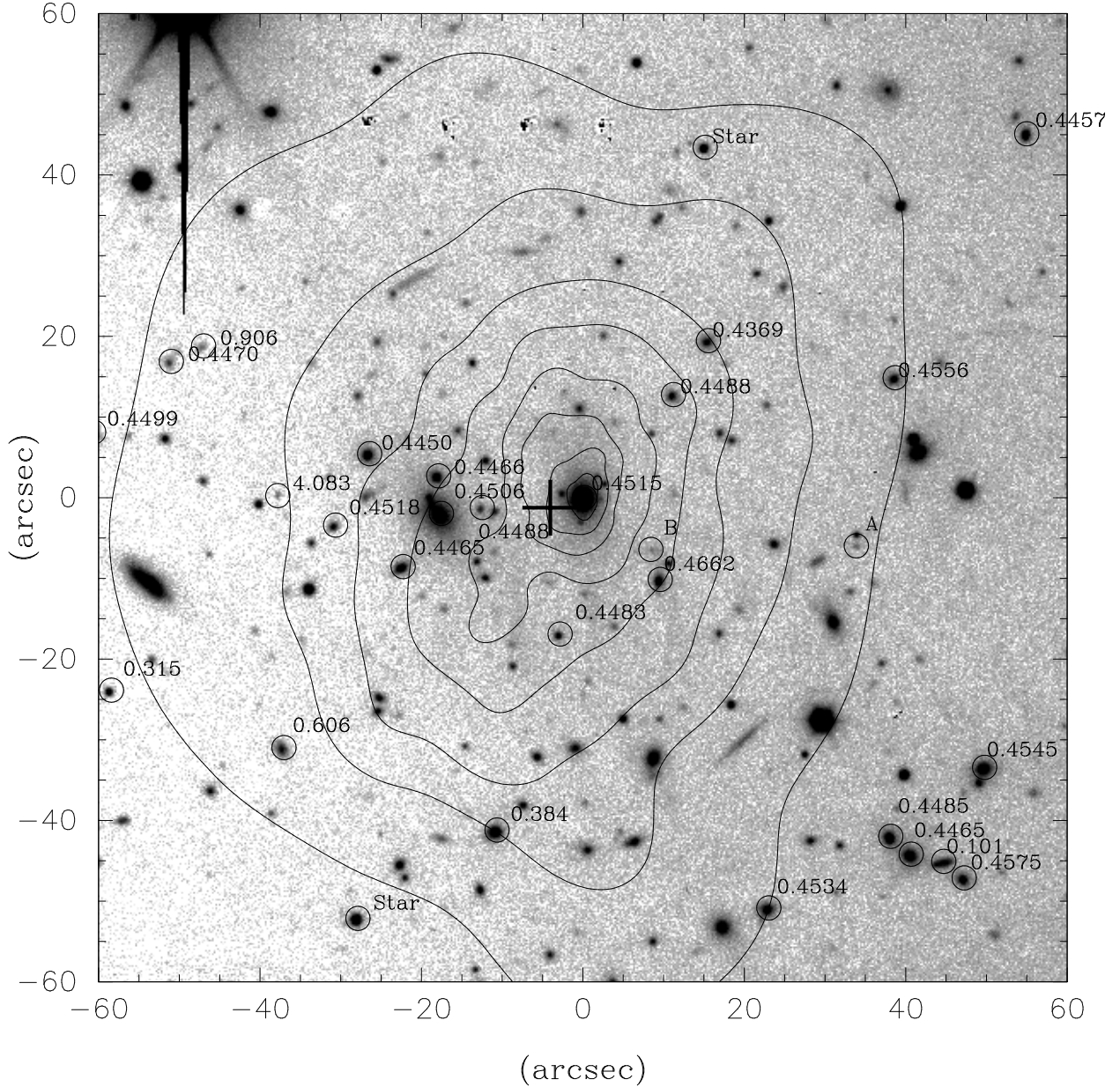


Fig. 2.— The R -band image of the central 2×2 arcmin 2 region of RX J1347–1145 is shown, with the *Chandra* smoothed X-ray surface-brightness contours (logarithmically spaced) overlaid. The objects in our spectroscopic sample are marked with their redshifts. We also marked the possible counter images (A and B) of the $z = 4.083$ object.

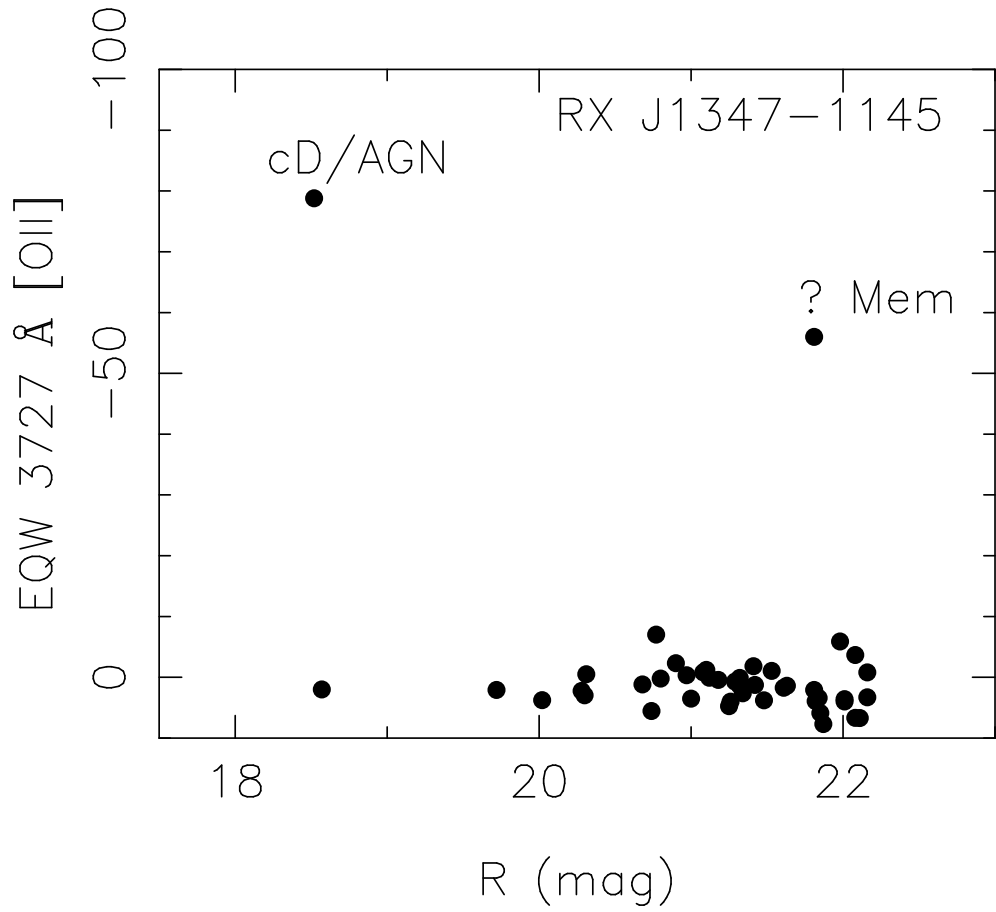


Fig. 3.— The rest frame equivalent width of the emission line of [OII] at 3727Å is shown as a function of total R mag for the sample of galaxies in the massive cluster RX J1347–1145. The central AGN and one possible non-member, marked on the figure, are the only galaxies in the sample with detectable emission in this line.

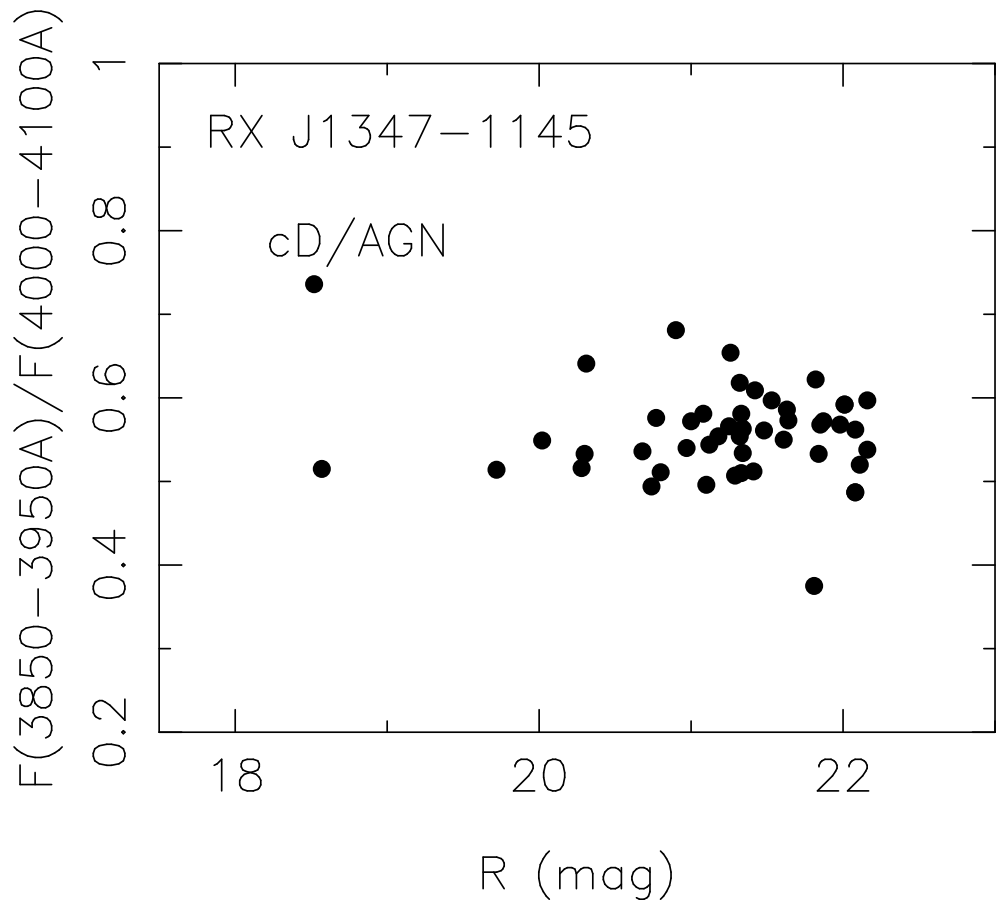


Fig. 4.— An index measuring the strength of the Balmer jump in the rest frame is shown as a function of total R mag for the sample of galaxies in the massive cluster RX J1347–1145. The value 1.0 corresponds to no discontinuity in the spectrum. The central AGN and one possible non-member, which has such a blue continuum that its Balmer discontinuity index exceeds unity, are the only anomalous galaxies in this plot.

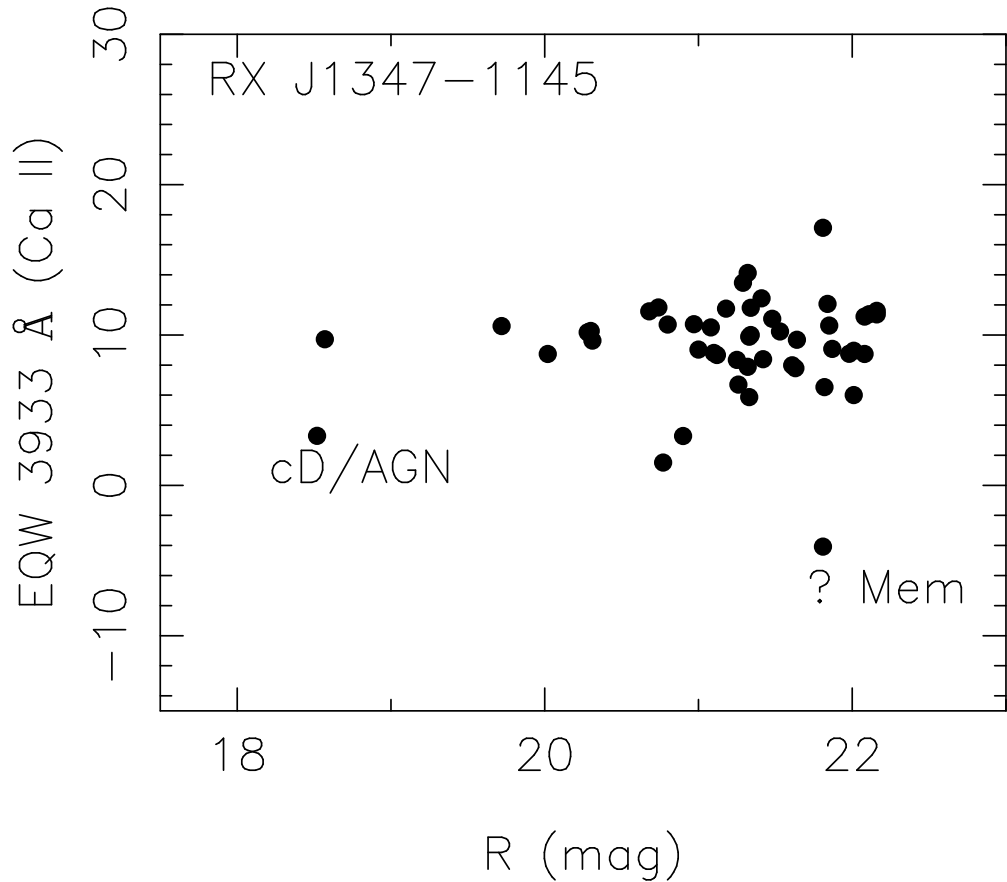


Fig. 5.— The rest frame equivalent width of the Ca II absorption line at 3933Å is shown as a function of total R mag for the sample of galaxies in the massive cluster RX J1347–1145. The central AGN and one possible non-member, marked on the figure, have anomalously weak absorption in this line.

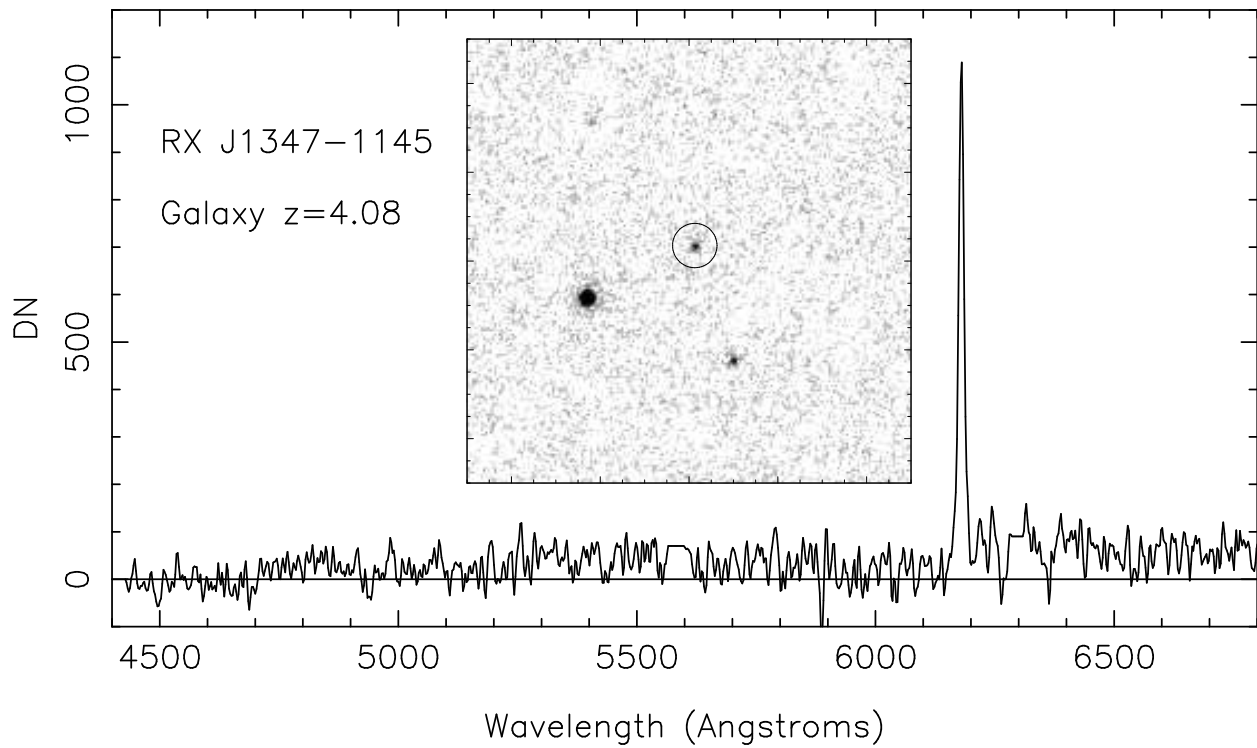


Fig. 6.— The spectrum of the $z = 4.083$ galaxy found near the center of the cluster of galaxies RX J1347–1145 is shown. The residuals from subtraction of the strong night sky lines at 5577\AA and at 6300\AA have been removed by setting the counts to a constant within those specific intervals. The superposed image is a zoom on the archival HST/STIS data showing the point source morphology of the object.